

## Symmetry Breaking in Boron Nitride Nanotubes

Masa Ishigami,<sup>1,2</sup> Jay Deep Sau,<sup>1,2</sup> Shaul Aloni,<sup>1,2,3</sup> Marvin L. Cohen,<sup>1,2</sup> and A. Zettl<sup>1,2,3,\*</sup>

<sup>1</sup>*Department of Physics, University of California at Berkeley, Berkeley, California 94720, USA*

<sup>2</sup>*Materials Sciences Division, Lawrence Berkeley National Laboratory, Berkeley, California, 94720, USA*

<sup>3</sup>*The Molecular Foundry, Lawrence Berkeley National Laboratory, Berkeley, California, 94720, USA*

(Received 13 January 2006; published 27 October 2006)

We have imaged boron nitride nanotubes with atomic scale resolution using scanning tunneling microscopy. While some nanotubes show the expected triangular lattice pattern, the majority of the nanotubes show unusual stripe patterns which break the underlying symmetry of the boron nitride lattice. We identify the origin of the symmetry breaking and demonstrate that conventional STM imaging analysis is inadequate for boron nitride nanotubes.

DOI: [10.1103/PhysRevLett.97.176804](https://doi.org/10.1103/PhysRevLett.97.176804)

PACS numbers: 73.22.-f

Boron-nitride nanotubes (BNNTs) are inorganic analogues of carbon nanotubes (CNTs) and possess physical properties suitable for a broad variety of applications [1]. BNNTs have a high Young's modulus [2] and are good thermal conductors [3] much like CNTs, but possess radically different electronic properties. Unlike CNTs, previous calculations [4,5] have shown that electronic properties of BNNTs are uniform and not dependent on their chiral angles or diameters [6]. Since there are no synthesis techniques to control chiral angles and diameters of CNTs, BNNTs are considered to be better suited for some electronics applications in which the uniform electronic property is desirable [7].

In this Letter, we report atomic scale features resolved on BNNTs using scanning tunneling microscopy (STM). Surprisingly, only 10% of nanotubes studied show the expected triangular lattice pattern while the majority appear with a stripe pattern which breaks the symmetry of the underlying hexagonal boron nitride lattice. We account for the symmetry breaking by analyzing the electron transport problem at the tunneling junction using detailed *ab initio* calculations.

The BNNTs used in this study were produced using an arc-discharge technique [8]. As-grown soot was then ultrasonically suspended in 1, 2-dichloroethane and deposited from the suspension on Au(111) surfaces. The nanotubes in our STM samples were mostly double walled with diameters of  $27 \pm 3$  Å as determined from transmission electron microscopy and atomic force microscopy. The samples were outgassed at 623 to 723 K for 3 hours in ultrahigh vacuum prior to the STM investigations. The experiment was performed using a homemade ultrahigh vacuum low-temperature STM operated at 7 K. We find that the BNNTs are less susceptible to imaging-induced damages at negative sample voltages.

Atomic scale features can be resolved only when the nanotubes appear cylindrical at sample bias voltages higher than 3 to 4 V. The noncylindrical appearance of the nanotubes at low bias voltages is due to the giant Stark

effect (GSE) [9,10]. Nominal height variations of these on-tube features are 0.2 Å. 10% of the nanotubes display the expected triangular lattice pattern with the approximate lattice constant of 2.5 Å as shown in Fig. 1. Figures 2(a)–2(c) show representative STM images of the stripe pattern which appears on the majority of the nanotubes. The periodicity of the stripe pattern is  $2.3 \pm 0.49$  Å. Orientation angles of the stripe pattern with respect to the axis of the nanotubes measured in the clockwise direction range from  $-41 \pm 9^\circ$  to  $+38 \pm 9^\circ$  [12]. The stripe pattern has no bias dependence and the nanotubes displaying the stripe pattern never display the triangular lattice pattern under varied tunneling parameters.

What is the origin of the broken symmetry in BNNTs? We have systematically ruled out anomalous tip shapes, and other extrinsic imaging effects as causes for the unusual patterns [14]. Instead, the double barrier electron transport [23] at the tunneling junction is responsible for the observed features. We show that the stripe patterns are due to the loss of the triangular symmetry in the tunneling current rather than in the local charge densities. In addition, the orientation angles of the stripe patterns are found to be the chiral angles of the BNNTs.

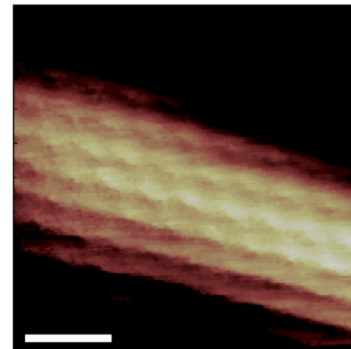


FIG. 1 (color online). Constant current STM image of a BNNT appearing with a triangular lattice pattern.  $V_{\text{sample}} = -4.8$  V and  $I_{\text{tunnel}} = 1.0$  nA.

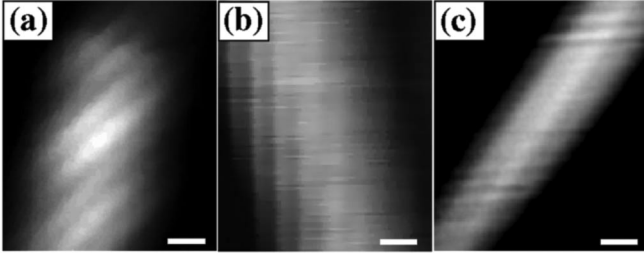


FIG. 2. Constant current STM image of BNNTs appearing with a stripe pattern. The scale bars are 5 Å in length. The stripe patterns are angled (a) +24°, (b) +9.2°, and (c) -1.6° with respect to the axis of nanotubes. Wave patterns appearing horizontal in (c) are due to noise. The images are acquired with (a)  $V_{\text{sample}} = -3.8$  V and  $I_{\text{tunnel}} = 0.2$  nA, (b)  $V_{\text{sample}} = -4.6$  V and  $I_{\text{tunnel}} = 0.75$  nA, and (c)  $V_{\text{sample}} = -4.8$  V and  $I_{\text{tunnel}} = 0.2$  nA.

The high sample bias voltages required to image the atomic scale features impose a local electric field sufficient to induce a significant GSE which is estimated to reduce the band gap to approximately 1 eV [9,11]. The Fermi level alignment of the tip, nanotube, and substrate allows electronic states, derived from both the valence and conduction band states near the electronic band gap, to participate in the tunneling process in this high field regime. Spatial distributions of these electronic states are significantly altered by the GSE. Electronic states are evenly distributed around the nanotube circumference at the zero sample bias voltage. With negative sample bias voltages, the valence band states are located near the substrate away from the tip and the conduction band states are located near the tip away from the substrate. Therefore, a proper calculation of STM images requires considering the tunneling probabilities of nanotube electronic states to both the tip and the substrate electronic states. The contribution to the tunneling current from a given electronic state in our calculations must be additionally weighted by a tunneling probability to the substrate unlike in the conventional STM calculations.

We account for the tunneling probability to the substrate by using the expression for the current through a double barrier tunneling junction in the weak tunneling limit [23,24]

$$I \propto \sum_n \Theta(\mu_{\text{tip}} - \epsilon_n) \Theta(\epsilon_n - \mu_{\text{substrate}}) \frac{\rho_{n,\text{tip}} \rho_{n,\text{substrate}}}{\rho_{n,\text{tip}} + \rho_{n,\text{substrate}}}, \quad (1)$$

where  $\Theta$  is the unit step function and  $\mu_{\text{tip}}$  and  $\mu_{\text{substrate}}$  are relative chemical potentials of the tip and the substrate. Chemical potentials of the tip, nanotube, and substrate are self-consistently determined by the procedure formally developed for the double barrier tunneling problem [25,26].

We have calculated theoretical STM images for (20,20) and (4,16) single-walled nanotubes. The STM images are

calculated using the density functional theory within the local density approximation. For the (20,20) nanotube the calculations are performed using a local combination of atomic orbitals (LCAO) with double zeta polarized basis in the SIESTA code. For the (4,16) nanotube we use a plane wave basis with real pseudopotential using the PARATEC code. Some of the conduction band states of a BNNT are nearly free electron like [4] and are poorly described by an LCAO basis. However, our calculations based on a plane wave basis find that these states redistribute to the close proximity of either the tip with negative sample bias voltages or the substrate with positive sample bias voltages and hence participate only weakly in the transport across the tunneling junction. Therefore, both of our calculation methods are sufficient for analyzing the experiment.

Our calculations find that STM images acquired with high negative sample bias voltages are dominated by the conduction band states at the bottom of the conduction band for both (20,20) and (4,16) nanotubes. These conduction band electronic states are located far from the substrate due to the GSE and cannot hybridize with the substrate electronic states [27]. Therefore, the conventional methods [28–34] for calculating STM images of substrate-hybridized adsorbates do not apply in the present problem. Figure 3(a) shows an unweighted STM image of a (20,20) nanotube calculated without including the tunneling probabilities to the substrate. The image displays a triangular lattice pattern which retains the underlying symmetry of the hexagonal boron nitride lattice. Therefore, the GSE does not disturb the triangular symmetry of the spatial distribution of the electronic states and the stripe patterns are not explained by the GSE alone. A weighted STM image calculated including the proper tunneling probabilities is shown in Fig. 3(b). A vertical stripe pattern, parallel to the nanotube axis with a periodicity of 2.17 Å, is clearly visible. The calculated image reproduces the stripe pattern seen in the experiment and is similar to what is shown in Fig. 2(c). For chiral BNNTs, stripe patterns also appear when the tunneling probabilities are included in the calcu-

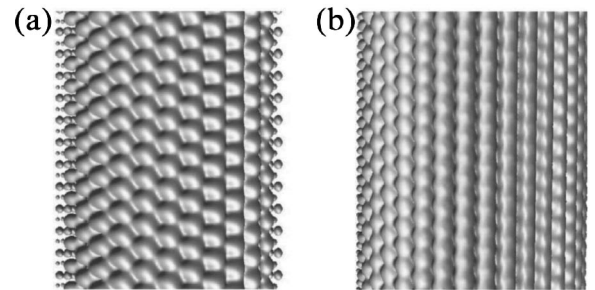


FIG. 3. (a) Unweighted tunneling image calculated for a (20,20) single-walled BNNT displaying a triangular lattice pattern. (b) Weighted tunneling image calculated for (20,20) single-walled BNNT displaying a vertical stripe pattern with a periodicity of 2.1 Å. Theoretical applied sample bias voltage is approximately -4 V.

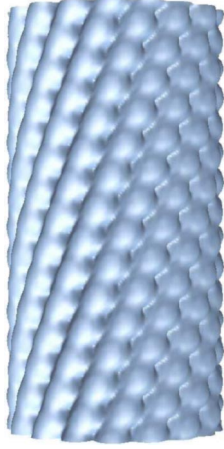


FIG. 4 (color online). Weighted tunneling image calculated for the tunneling probability for a (4,16) single-walled BNNT showing a stripe pattern angled  $19.1^\circ$  from the tube axis. The calculation was performed with a theoretical sample bias voltage of  $-4$  volts.

lation. The orientation angle of a stripe pattern is the same as the chiral angle of a given nanotube. Figure 4 shows our weighted theoretical STM image for the (4,16) nanotube displaying a stripe pattern oriented at  $19.1^\circ$  from the nanotube axis which is the same as the chiral angle. Thus, for nanotubes shown in Figs. 2(a)–2(c), the chiral angles are  $24^\circ$ ,  $9.2^\circ$ , and  $-1.6^\circ$ .

The mechanism for the appearance of stripe patterns in weighted theoretical STM images can be explained using the zone folding approach. Figure 5 shows the first Brillouin zone for a sheet of hexagonal boron nitride. Conduction band minima are at  $\Gamma$ ,  $M$ , and  $K$ . The nearly free electron state discussed previously is at  $\Gamma$ . There are 2  $K$  points ( $K = (1/3, 2/3)$  and  $\bar{K} = (2/3, 1/3)$ ) and 3  $M$  points which we call  $M_1 = (0, \pm 1)$ ,  $M_2 = (\pm 1, 0)$ , and  $M_3 = \pm(1/2, 1/2)$ . The STM tip-induced electric potential on the tube is given by  $V(\theta) = V_0 \cos(\theta)$ , where  $\theta$  is the circumferential coordinate of nanotubes. This slowly varying electric field confines electronic states in the direction of the tip-induced electric field along the wrapping vector for a nanotube. Using the Wentzel-Krammer-Brillouin method, the decay length of a state being confined by this potential is proportional to  $1/\sqrt{m_{\text{eff}}}$ , where  $m_{\text{eff}}$  is the effective mass of the state in the direction of the applied electric field. Effective masses at  $M$  points are smaller than those at  $\Gamma$  and  $K$  points. Furthermore, the lightest effective mass is found to be in the direction towards the  $\Gamma$  point at the  $M$  points. Since the applied electric field is most parallel to the  $M_3$  to  $\Gamma$  direction, the electronic state at the  $M_3$  point is the most dominant contributor to the tunneling current.

As calculated by both the PARATEC and the SIESTA code, the tunneling current at high negative bias voltages is derived primarily from the conduction band states. These conduction band states originate from  $p_z$  orbitals of boron

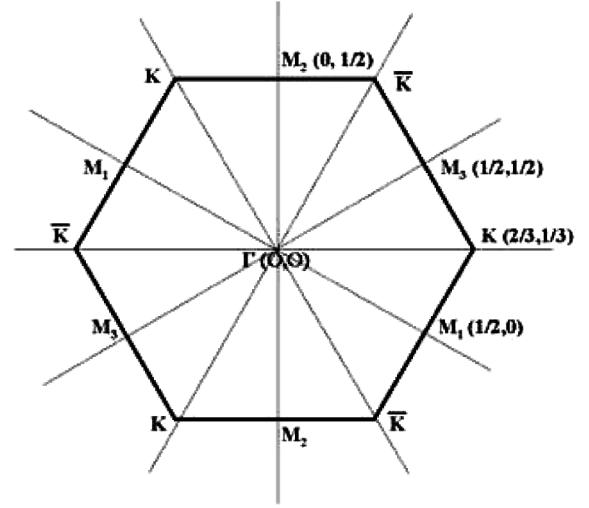


FIG. 5. Hexagonal first Brillouin zone of a sheet of hexagonal boron nitride.

atoms. There are six nearest neighbor boron atoms to a given boron atom, “A”, located at  $(0,0)$ . These atoms can be grouped into 3 sets of atoms located at  $P_1 = (\pm a, 0)$ ,  $P_2 = (0, \pm a)$ , and  $P_3 = (\pm a, \mp a)$ , where  $a$  is the lattice constant of hexagonal boron nitride. Boron  $p_z$  orbitals at the  $P_3$  point are related to the electronic state at the  $M_3$  point in the momentum space. The intensity of a bond between  $A$  and  $P_3$  is proportional to

$$|1 + e^{i(k_1 x_1 + k_2 x_2)}|^2 = 2[1 + \cos(k_1 x_1 + k_2 x_2)], \quad (2)$$

where  $(k_1, k_2)$  is the coordinate in the momentum space for the  $M_3$  point and  $(x_1, x_2)$  is the coordinate in the real space for the  $P_3$  atoms. Equation (2) shows that the  $M_3$  state interferes constructively producing a stripe pattern which connects  $A$  and  $P_3$  atoms. The orientation angle is given by

$$\sin(\phi) = \frac{n - m}{2\sqrt{m^2 + n^2 + mn}}, \quad (3)$$

where  $\phi$  is the angle relative to the tube axis. The angle coincides with the chiral angle of nanotubes [35]. Equation (3) dictates that the angle should be between  $-30^\circ$  and  $+30^\circ$ , consistent with the experimental observation.

The stripe patterns, appearing on 90% of the BNNTs, are due to the combination of the GSE and the tunneling probabilities of each electronic state to the substrate. If there are conducting impurities present in the tunneling junction and these tunneling probabilities can be disregarded, the triangular lattice patterns are seen instead.

This work was supported in part by the National Science Foundation under Grants No. DMR-9801738, No. DMR-9501156, and No. DMR00-87088 and by the Director, Office of Energy Research, Office of Basic Energy Sciences, Division of Materials Sciences of the U.S. Department of Energy under Contract No. DE-AC03-

76SF00098 within the  $sp^2$  Nanomaterials Program. We thank NERSC and SDSC for providing supercomputer time to perform the calculations. M.I. acknowledges the support of the Hertz Foundation.

\*Electronic address: azettl@socrates.berkeley.edu

- [1] R. Tenne and A. Zettl, in *Carbon Nanotubes: Synthesis, Structure, Properties, and Application*, edited by M. S. Dresselhaus, G. Dresselhaus, and P. Avouris, Topics in Applied Physics, Vol. 80 (Springer-Verlag, New York, 2001), p. 83.
- [2] N. G. Chopra and A. Zettl, *Solid State Commun.* **105**, 297 (1998).
- [3] C. Chang, W.-Q. Han, and A. Zettl, *J. Vac. Sci. Technol. B* **23**, 1883 (2005).
- [4] A. Rubio, J. L. Corkill, and M. L. Cohen, *Phys. Rev. B* **49**, 5081 (1994).
- [5] X. Blase, A. Rubio, S. G. Louie, and M. L. Cohen, *Europhys. Lett.* **28**, 335 (1994).
- [6] BNNTs with smaller diameters are predicted to have narrower band gaps, but these diameters are not experimentally seen
- [7] M. Radosavljevic, J. Appenzeller, V. Derycke, R. Martel, P. Avouris, A. Loiseau, J. L. Cochon, and D. Pigache, *Appl. Phys. Lett.* **82**, 4131 (2003).
- [8] J. Cumings and A. Zettl, *Chem. Phys. Lett.* **316**, 211 (2000).
- [9] K. H. Khoo, M. S. C. Mazzoni, and S. G. Louie, *Phys. Rev. B* **69**, 201401 (2004).
- [10] The GSE, induced by the applied local electric field of the STM tip, shifts the spatial distribution of electronic states in the BNNTs. As a result, only electronic states located near the substrate can contribute to the tunneling current at lower sample bias voltages and the nanotubes appear as noncylindrical, “rain gutter”-like, structures in STM images [11]. Atomic scale features on the top of nanotubes deposited on the substrate, accessible by the STM tip, can only be resolved when the nanotubes appear cylindrical at higher sample bias voltages.
- [11] M. Ishigami, J. Sau, S. Aloni, M. Cohen, and A. Zettl, *Phys. Rev. Lett.* **94**, 056804 (2005).
- [12] The angles for these stripe patterns are determined by using the procedure determined in [13] from STM images. Raw data from the images are (a)  $+30.9^\circ$ , (b)  $+12.5^\circ$ , and (c)  $-2^\circ$ .
- [13] L. C. Venema, V. Menueir, P. Lambin, and C. Dekker, *Phys. Rev. B* **61**, 2991 (2000).
- [14] In addition, we have also ruled out other possible structural and electronic origins for the stripe pattern. Gas molecules are expected to desorb at lower temperatures than degassing temperatures prior to our experiments [15–17]. Moiré pattern formed by the inner and outer layers of the nanotubes cannot produce sufficiently small periodicities to explain the stripe pattern [18,19]. Finally the degenerate electronic states [20,21], which interfere with each other to form the similar pattern in STM images of carbon nanotubes, do not exist in the BNNTs [22].
- [15] W. Xiaojun, J. Yang, J. Hou, and Z. Qingshi, *Phys. Rev. B* **69**, 153411 (2004).
- [16] W. Xiaojun, J. Yang, J. Hou, and Z. Qingshi, *J. Chem. Phys.* **121**, 8481 (2004).
- [17] J. Seung-Hoon and K. Young-Kyun, *Phys. Rev. B* **69**, 245407 (2004).
- [18] J. Xhie, K. Sattler, M. Ge, and N. Venkateswaran, *Phys. Rev. B* **47**, 15 835 (1993).
- [19] G. Maohui and K. Sattler, *Science* **260**, 515 (1993).
- [20] W. Clauss, D. Bergeron, M. Freitag, C. Kane, E. Mele, and A. Johnson, *Europhys. Lett.* **47**, 601 (1999).
- [21] C. Kane and E. Mele, *Phys. Rev. B* **59**, R12 759 (1999).
- [22] Y.-H. Kim, K. J. Chang, and S. G. Louie, *Phys. Rev. B* **63**, 205408 (2001).
- [23] S. Datta, *Electronic Transport in Mesoscopic Systems* (Cambridge University Press, Cambridge, England, 1995).
- [24] H. Birk, M. de Jong, and C. Schonenberger, *Phys. Rev. Lett.* **75**, 1610 (1995).
- [25] S. Datta, W. Tian, S. Hong, R. Reifengerger, J. Henderson, and C. P. Kubiak, *Phys. Rev. Lett.* **79**, 2530 (1997).
- [26] W. Tian, S. Datta, S. Hong, R. Reifengerger, J. Henderson, and C. P. Kubiak, *J. Chem. Phys.* **109**, 2874 (1998).
- [27] It is important to note that, in addition, the tip is located  $5 \text{ \AA}$  [11] away from the nanotubes and the tip electronic states do not hybridize either with the nanotube electronic states, which are important for the transport across the nanotube.
- [28] M. Gata and P. Antoniewicz, *Phys. Rev. B* **47**, 13 797 (1993).
- [29] V. Hallmark and S. Chiang, *Surf. Sci.* **329**, 255 (1995).
- [30] F. Biscarini, C. Bustamante, and V. Kenkre, *Phys. Rev. B* **51**, 11 089 (1995).
- [31] P. Sautet and M.-L. Bocquet, *Phys. Rev. B* **53**, 4910 (1996).
- [32] J. Nieminen, E. Niemi, and K.-H. Rieder, *Surf. Sci.* **552**, L47 (2004).
- [33] J. A. Stroscio and W. J. Kaiser, *Scanning Tunneling Microscopy* (Academic, San Diego, 1993).
- [34] R. Wiesendanger, *Scanning Probe Microscopy and Spectroscopy* (Cambridge University Press, Cambridge, England, 1994).
- [35] In  $(n, 0)$  nanotubes,  $M_3$  and  $M_1$  states are equivalent and two stripe patterns angled  $60^\circ$  from each other should appear simultaneously.